

# COMPREHENSIVE STUDY OF SOLAR CELL STRUCTURE DEFECTS BY MEANS OF NOISE AND LIGHT EMISSION ANALYSIS

Robert MACKU<sup>1</sup>, Pavel KOKTAVY<sup>1</sup>, Jiri SICNER<sup>1</sup>

<sup>1</sup>Department of Physics, Faculty of Electrical Engineering and Communication, Brno University of Technology  
Technicka 8, 616 00 Brno, Czech Republic

macku@feec.vutbr.cz, koktav@feec.vutbr.cz, xsicne02@stud.feec.vutbr.cz

**Abstract.** This paper discusses the issue of silicon solar cells localized defects from metrological and physical points of view. Structure imperfections represent the real problem because of solar cells long-term degradation and conversion efficiency decreasing. To this aim we pay our attention to research relating to the defect light emission and correlation with rectangular microplasma fluctuation. A sensitive CCD camera has been used for mapping of surface photon emission. The operation point of the samples has been set to reverse bias mode, and different electric field intensity was applied. We managed to get interesting information using a combination of optical investigation and electrical noise measurement in time and spectral domain. It will be revealed that a direct correlation between noise and photon emission exists and the results related to several defect spots are presented in detail in this paper.

## Keywords

*Electric noise, light emission, local defect, solar cell.*

## 1. Introduction

Numbers of technologically different solar cells have been touted as the most promising solution for the cost-effective green energy source. This is partly due to the advantages of different technological approaches suitable for different applications. The main parameters in a view are related to efficiency, cost or deposition rate, long-term stability in outdoor testing and impact on the environment. Despite to the level of effort on innovations of manufacturing processes, there is a huge discrepancy between the laboratory and industry based solar cells. The main problems are related to efficiency and defects reducing life-time. This is compounded by a lack of comprehensive scientific bases for interpretation of specific defect in the structure partly due to the large scale manufacturing process and new materials. This lack of systematic science base has been the biggest hindrance

to progress in the photovoltaics and innovations have been often empirical. Our aim is to suggest physical interpretation of local defects and bulk inhomogeneities taking place in the samples. Currently, we focus mainly on single-crystal silicon solar cells because of good level of silicon condensed matter physics. Partially we also attend to Cu(InGa)Se<sub>2</sub> solar cells with the same aim, but it would not be presented in this paper. We introduce electrical noise measurement as a tool for electrical stress detection, transport characteristic measurement to study charge transfer and breakdown effects and optical radiation measurement in order to characterize pre-breakdown and/or breakdown phenomena.

## 2. Samples under Investigation

Experiments will be carried out here with conventional types of solar cells. These samples have a traditional pyramidal surface texture. Thanks to an appropriate texture and multiple reflections better radiation absorption is achieved. Moreover, depletion region position is optimized in view of silicon absorption coefficient to collect energetic radiation and it is close to the surface. The cross section of the solar cell sample is depicted in Fig. 1. This approach makes solar cells very sensitive to texturization imperfections and mechanical damage. That is why it is very important to keep attention to the microscopy topography image. We use both SEM and lesser-known SNOM (Scanning Near-field Optical Microscope) microscopes. Typical texturization is depicted in Fig. 2. There are no apparent mechanically induced imperfections.

The *pn* junction is localized close to the surface and traces pyramidal texturization. The depletion layer width is about of 0,6  $\mu\text{m}$  (without the applied bias voltage). The solar cells are made from single-crystal silicon and have the dimensions 12×12 cm and a thickness of 230  $\mu\text{m}$ . Nevertheless, only small-scale fragments will be studied here to avoid enormous number of presented defects. The *p* and *n* layers are formed by diffusion. The *p* type substrate is made by the

Czochralsky process with the resistivity of about  $1,2 \Omega \cdot \text{cm}$ . A silicon nitride layer with the thickness of about 78 nm, which is laid on the cell surface, is intended to passivate the silicon surface and also reduces the reflection losses. The cells are designed for the solar panel fabrication. The screen-printed silver paste metallization was used for contacts on the front side. The back side of the solar cells has a structure of Al BSF with Ag/Al busbars.

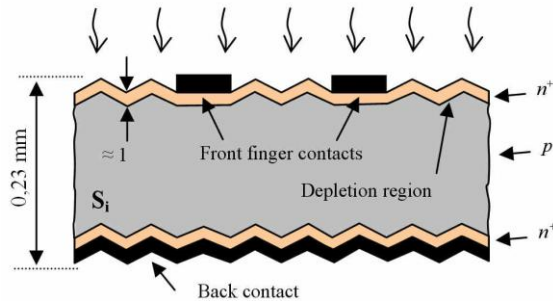


Fig. 1: Principal silicon solar cell cross-section.

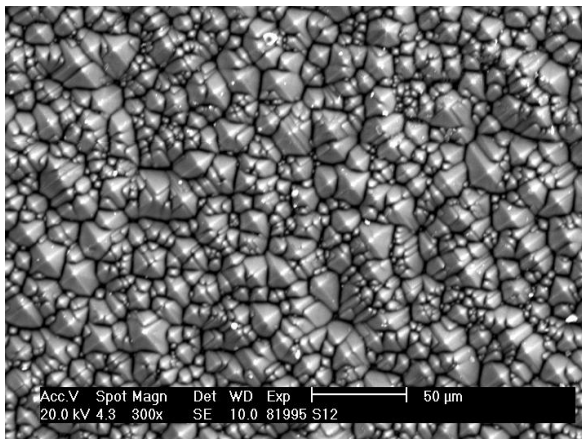


Fig. 2: Solar cell surface topography image, scanning electron microscope SEM.

### 3. Experimental Details

#### 3.1. Electric Noise Measurement

It is typical for solar cells that the nature of the observed noise depends on the voltage applied to them. This can be attributed to variations in the electric stress and breakdowns origin. This is why our study is divided into reverse and forward -bias conditions. With regard to the local defect inspection, all above reverse-biased solar cells will be studied. The solar cell bias voltage is provided by a high-precision laboratory power supply. Its output voltage must be filtered because of additive noise types presence. The filter cut-off frequency is approx. 1 Hz. The specimen under investigation is placed in the dark environment, is electrically shielded and is kept at a constant temperature  $(16,6 \pm 0,2) ^\circ\text{C}$  to avoid self-heating. A pick-up resistor  $R_L$  to measure the specimen

current fluctuations, is connected in series with the specimen ( $R_L = 5,36 \Omega$ ). The simplified circuit diagram is depicted in Fig. 3. The noise voltage is amplified by means of low-noise amplifiers (PA31 – gain 20 dB, cut-off frequency 10 MHz; EG&G 5113 – gain 30 dB, cut-off frequency 1 MHz) and measured by means of selective nanovoltmeter (Signal Recovery Model 7310) or alternatively by FFT dynamic spectral analyzer Agilent 35670A. From the procedure viewpoint, the approach remains the same in both cases. The noise nature will be appraised on the basis of the measurements of the double-sided noise power spectral density (PSD).

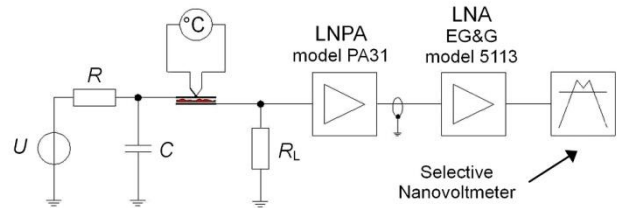


Fig. 3: Simplified circuit diagram of the experimental arrangement for noise measurement. Here U is the bias voltage supply, LNPA is the low-noise pre-amplifier, LNA is the low-noise amplifier.

#### 3.2. Light Emission Measurement

Radiation generated from reverse-biased *pn* junction defects is used to study local properties (far field detection). It proves to be useful to measure surface radiation and to make light spots localization also to measure the radiation intensity versus voltage plot, its correlation with other, mainly noise characteristics and radiation spectrum. To this aim a scientific CCD camera G2-3200 with a 3,2 MPx resolution was used for measuring of radiation from a *pn* junction solar cell surface. It uses a silicon chip cooled by dual system of Peltier's modules with the operation temperature down to  $-50 ^\circ\text{C}$ . The Dark current of an optical sensor and a single pixel is  $0,8 \text{ e} \cdot \text{s}^{-1}$  (it holds for  $T = 0 ^\circ\text{C}$ ). The dynamic range of the elementary pixels with a usable range up to 16 bits is very good. The camera lens with a focal ratio 1,2 and working aperture 41,7 mm is used with the camera. It is possible to measure in a useful range of wavelengths of 300 nm – 1100 nm. Since the producer defines the spectral characteristics of the particular CCD chip, photometry measurements can be performed as in our case. Optical filters are included to an optical path to obtain the spectral characteristics. FWHM (Full Width at Half Maximum) of the regular filters is 150 nm and their optical response is calibrated. It is possible to include interference filters with FWHM of about 10 nm ahead of the lens. Detected radiation is relatively weak due to its high selectivity and this measurement is very technically and time consuming. The calibration is not performed separately for each of these filters, but measurement is carried out with the average spectral transmission function. The results are therefore correct in principle, but we work with them in relative terms.

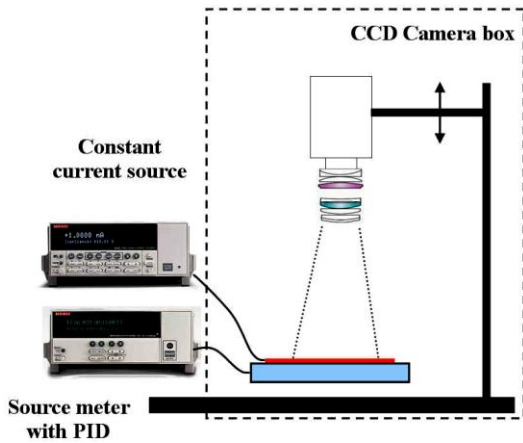


Fig. 4: Experimental set-up for light emission measurement.

The CCD Camera together with the solar cell sample is in the optically shielded chamber (see Fig. 4). The sample temperature is kept constant during the measurement by the PID temperature regulator integrated in the Keithley source meter. The sample bias is realized by constant voltage source controlled via IEEE 488.2 bus.

## 4. Results and Discussions

### 4.1. Electric Noise at Avalanche Breakdown and Microplasma Region

The noise diagnostics is based on the assumption that the device structure defects give rise to excess noise. We can observe a number of different noise sources and their superposition respectively. In many cases, the stationarity is questionable and physical nature is not evident. In addition, noise develops its character with the applied DC voltage, see [1], [2], [3]. The noise experimental method has been put into connection with the optical surface observation and the photon emission detection. Thanks to that, we are able to distinguish the defect contributions from each other even in case the device contains a number of field activated defects [4], [1].

The first significant noise type, so-called microplasma noise, usually appears at sufficiently high reverse voltage lower than the breakdown voltage of the complete defect-free junction regions. It is caused by avalanche ionization breakdown in bistable form, more in [1], [5]. Figure 5 depicts microplasma current noise fluctuation in the time domain. This type of defects is directly connected with technological imperfections (impurities, dislocations, dopand concentration fluctuation) and it is possible to determine internal temperature, [6], and geometry [7].

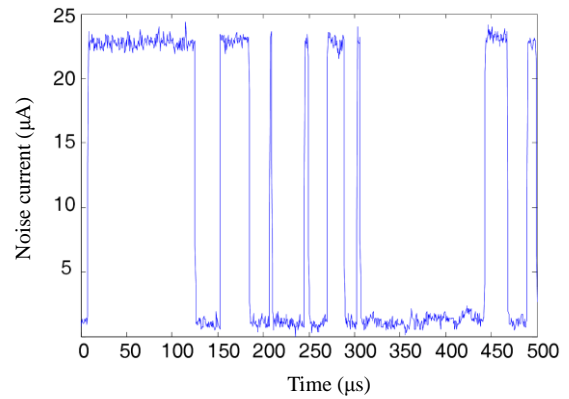


Fig. 5: Microplasma noise waveform, sample K20, reverse voltage  $U_R = 9,81$  V.

Spectral analyses show that the current noise power spectral density, which depends on the reverse voltage, is in a form of generation-recombination noise for the microplasma noise source, see Fig. 6. Since other local inhomogenities in a *pn* junction of the presented sample do not exhibit strong voltage dependence in the spectral domain, it is not possible to distinguish another particular noise sources. The current noise power spectral density is in a form of  $1/f$  noise for the reverse voltage out from the microplasma instability region and pointed out rather thermal unstable mechanism. It corresponds to the non-field activated process (spot 1) as presented thereafter. Then  $1/f$  fluctuations may mask another noise sources.

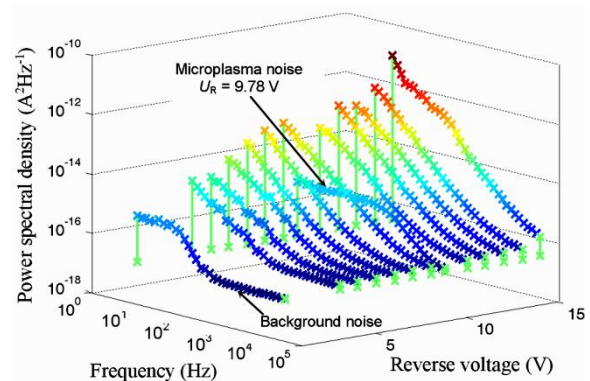


Fig. 6: Current noise power spectral density for various reverse voltages, sample K20, temperature 16,6 °C.

Interpretation of the  $1/f$  noise and the explanation how different parts of the sample contributes are extremely complicated issue. More information is possible to find in literature as [2]. We confine ourselves to state that this phenomenon represents bulk imperfections and does not contribute to the local light emission. Note that the avalanche multiplication (or impact ionization) has a positive temperature coefficient for breakdown. Due to this fact, we may discriminate avalanche multiplication (or microplasma noise) from e.g. tunneling effect or thermal instability by means of the current-voltage characteristic measurement. On behalf of phenomenon properties conversation, it is necessary to keep the temperature of the solar cell sample constant

during the measurement.

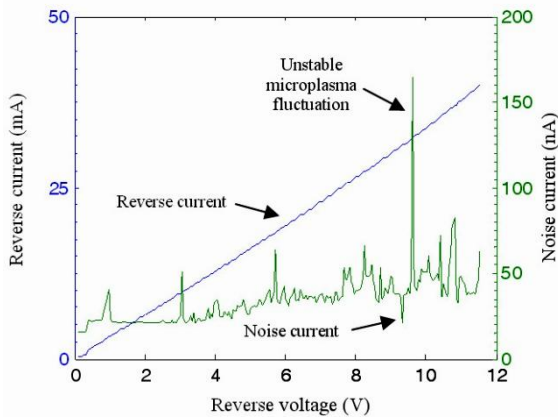


Fig. 7: Narrowband noise signal and DC current for various reverse voltages, sample K20,  $T = 28\text{ }^{\circ}\text{C}$ .

Another non-destructive method which we use for microplasma identification is based on the fact that the generation-recombination spectrum doesn't have the neglectable power in a frequency region where other noise are neglectable. We can measure narrowband noise signal (current signal) in the center frequency e.g. 1 kHz (see Fig. 7). We use the selective nanovoltmeter with high selectivity and effective bandwidth of about 30 Hz (the effective bandwidth is sometime called the noise bandwidth). The effective value of narrowband signal is measured via a DC voltmeter. Figure 7 depicts this experimentally obtained narrowband signal. It is interesting to see that microplasma regions are very closely bounded although bias current increase is about  $25\text{ }\mu\text{A}$  (far below apparatus resolution). Smaller peaks of noise characteristic (Fig. 7) indicate another type of noise or instabilities and they are not completely explained still. The second curve in the Fig. 7 represents reverse current vs. reverse voltage and we can conclude resistive-like sample behaviour in the broad sense.

#### 4.2. Radiation from Defect Spots and Correlation with Avalanche Breakdown and Microplasma

We study light emission by means of the CCD camera over the sample surface. Figure 8 depicts a fragment of the solar cell K20 with five defect spots emitting the light. It should be emphasized here that the photon emission intensity of the light spots depends on the applied voltage and some of them are suddenly activated with the increasing DC electric field (such as microplasma). Figure 8 represents high contrast photography of the solar cell after dual exposition in the dark and with bias light.

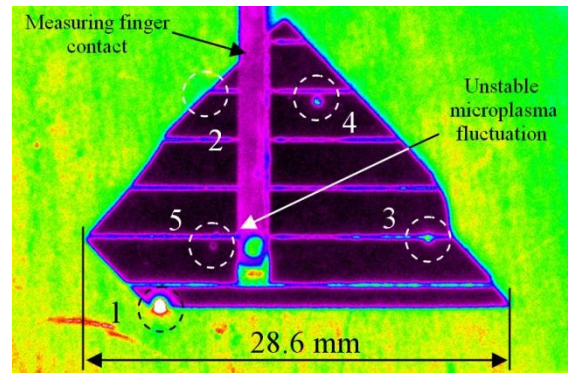
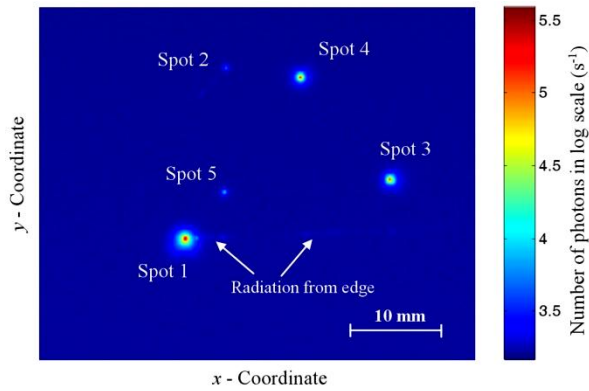


Fig. 8: Photography of measured solar cell with light spots, sample K20, reverse voltage 10 V.

Light spots represent, in general, local fluctuations of the *pn* junction width and the potential barrier width. It leads to decreasing of the breakdown voltage and local breakdown (conductive channels) may be created, [8], [1]. The local conductive channels concentrate the current from the neighbourhood and heavy current densities affect a low dimension region. This phenomenon can give rise to a heavy local temperature increasing and, consequently, local diffusion or thermal breakdown, which may result in the solar cell destruction. That is why it is extremely important to avoid this degradation.

The first light generation (see spot 1, Fig. 9) was detected at the sample edge for the reverse voltage from about 4 V. We suppose that the light generation for this case does not evoke by avalanche breakdown with respect to low value of the reverse voltage and the detection limit of the CCD camera. It is clear from the electrical measurements that the last light spot (spot 5) relates to the microplasma noise (Fig. 9) and it is caused by local avalanche breakdown. Light generation from this spot starts from the reverse voltage of 9,7 V which correlates very well with a narrowband noise signal (Fig. 7) and power spectral density (Fig. 6).

Regardless of aforementioned microplasma we expect another two fundamental defect types. It is a tunneling through a potential barrier defects and thermal instability defects. Let us consider the localized regions in a semiconductor material where conductivity is higher comparing to the neighbourhood. Naturally, the current will flow first of all through these regions. Consequently local lattice heating leads to thermal instabilities and breakdown. It should be noted here, that avalanche breakdowns may not necessarily generate current fluctuations. That is why we study thermal properties of defects light emission [10]. We were able to show that the presence of the tunneling phenomena is very unlikely. With regard to the sample noise activity the avalanche process plays the role here.



**Fig. 9:** Edge radiation and light spots with their intensity after avalanche breakdown in spot 5, sample K20, reverse voltage  $U_R = 10$  V.

Further information is possible to obtain from optical spectrum measurement. Figure 10 depicts optical spectrum again for individual light spots. It should be noted here, that the spot 2 was excluded from the measurement because of weak radiation intensity.

The measurement has been done using accurate interference filters included into the optical path. Optical filters properties (FWHM and insertion loss) weakly fluctuate with the center wavelength. On this account results are presented in relative units and as a reference point the spot 1 at 1100 nm was chosen. An interesting fact is that although the spot 1 (on the edge) has been created definitely mechanically optical spectrum of all light spots is very similar. The SEM picture of the spot 1 is in Fig. 11. Other mechanical imperfections related to the light spots have not been found yet.

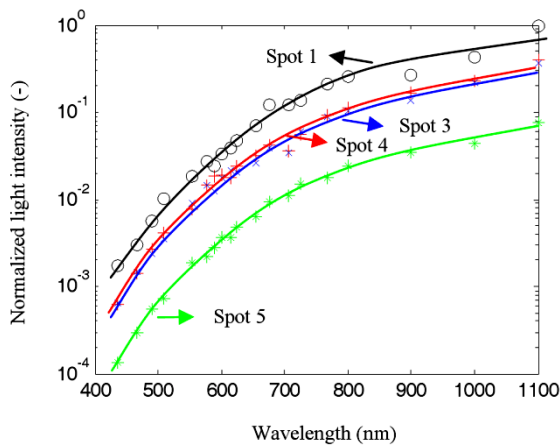


**Fig. 10:** Normalized light intensity versus wavelength, FWHM is about 10 nm, reference value at 1100 nm and spot 1, sample K20, reverse voltage 13,4 V.

Microscopy based study of defective areas is not easy way because we are not able to decide in advance whether an area is accompanied by topographic anomalies or not. On the contrary, microplasma defects induce radiative recombination in charge space region and the topography modification is not expected.

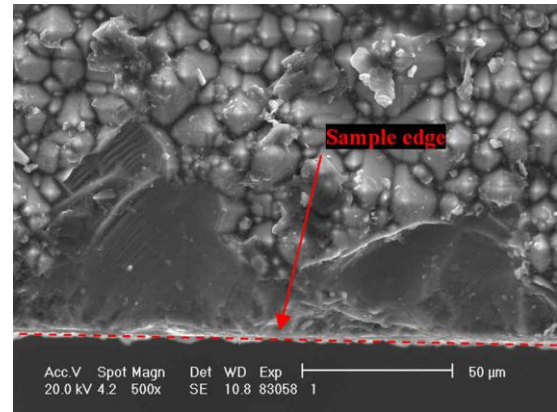


**Fig. 11:** SEM picture of spot 1.

The special part of our study is related to the repeatability of measurements because of defect modification by self heating. The defect structure or surrounding semiconductor properties could be modified and non-destructive conditions are not satisfied. That is why we use low level of the bias current or voltage and samples must be kept at the constant temperature. Figure 12 depicts the photon emission profile of the microplasma spot 5 for different reverse voltage. Radiation is probably generated below the surface in this case and the photon flux diffuses to a broad area. It creates a false impression that the defective area enlarges with the applied bias voltage.

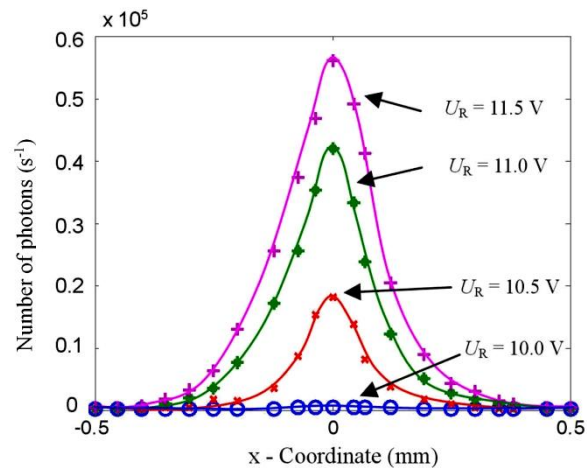


**Fig. 12:** Profile of optical radiation - microplasma defect spot 5 for different bias voltage  $U_R$ .

## 5. Conclusion

The mechanism of a reverse-biased junction conductivity appears to be due to the crystalline lattice (structural) imperfections, dislocations, or metallic precipitates in the *pn* junction region. Local breakdowns will thus take place in the neighbourhood of such defects at reverse voltages below those required for a breakdown in a defect-free region of the junction. Diagnostics of defected areas have been done by several methods which are measurement of current-voltage characteristics, measurement of RMS

value of narrowband current noise at reverse current or voltage, measurement of noise power spectral density, measurement of the radiation emitted from the defect during micro-plasma discharge formation. The latter method is applicable to optoelectronic devices and solar cells as presented in this paper.

The theoretical description of the photon spectrum emitted from defects spots is still an issue. Although silicon has indirect band structure the most probable process is band-to-band luminescence process at 1100 nm. The second expected mechanism of luminescence is generated by radiation via traps assisted recombination (impurities and mechanical defects) at ~ 1400 nm, [9]. Nevertheless, what we measure is a breakdown radiation due to impact ionization and avalanche multiplication. In this case, electrons are accelerated by the electric field from  $p$  to  $n$  type semiconductor. Local regions become conductive in the reverse direction. The electron kinetic energy or the velocity has broad statistic distribution. On this account, inter-band recombination forms broad photon emission. The avalanche current typically decreases with the increasing temperature because of the limiting kinetic energy by collisions with the crystal lattice. This approach was proved by the measurement of the temperature dependence of light emission. We also managed to find that the most local defects of solar cells are caused by this phenomenon.

## Acknowledgements

This paper is based on the research supported by the Grant Agency of the Czech Republic, the grant No. P102/10/2013, on the research supported by the Ministry of Industry and Trade of the Czech Republic, the project MPO TIP FR-TI1/305 and on the SIX research centre - project registration number: CZ.1.05/2.1.00/03.0072. International cooperation project LH11060 was also used. Authors wish to thank for this support.

## References

- [1] KOKTAVY, Pavel, Petr PARACKA and Ondrej KRCAL. Microplasma noise as a tool for PN junctions diagnostics. *WSEAS Transactions on Electronics*. 2008, vol. 4, no. 9, pp. 186-191. ISSN 1109-9445.
- [2] MACKU, Robert and Pavel KOKTAVY. Analysis of fluctuation processes in forward-biased solar cells using noise spectroscopy. *Physica status solidi (a)*. 2010, vol. 207, iss. 10, pp. 2387-2394. ISSN 1862-6319.
- [3] CHOBOLA, Zdenek. Noise as a tool for non-destructive testing of single-crystal silicon solar cells. *Microelectronics Reliability*. 2001, vol. 41, iss. 12, pp. 1947-1952. ISSN 0026-2714.
- [4] MACKU, Robert and Pavel KOKTAVY. Study of solar cells defects via noise measurement. In: *31st International Spring Seminar on Electronics Technology*. Budapest: IEEE, 2008, pp. 96-100. ISBN 978-1-4244-3972-0.
- [5] MCKAY, K.; G. Avalanche Breakdown in Silicon. *Physical Review*. 1954, vol. 94, iss. 4, pp. 877-884. ISSN 0031-899x.
- [6] KOKTAVY, Pavel, Robert MACKU, Tomas TRCKA and Bohumil KOKTAVY. Study of defect regions local heating in solar cells pn junctions by means of microplasma noise. In: *25th European Photovoltaic Solar Energy Conference*. Valencia: WIP-Renewable Energies, 2010, pp. 364-368. ISBN 3-936338-26-4.
- [7] MACKU, Robert and Pavel KOKTAVY. Vyziti mereni CU charakteristik pro urceni geometrie a polohy pn prechodu kremikových solarnich clanku. *Jemna mechanika a optika*. 2009, vol. 54, no. 10, pp. 291-293. ISSN 0447-6441.
- [8] LEVINSHTEIN, M. J. KOSTAMOVARA and S. VAINSHTEIN. *Breakdown Phenomena in Semiconductors and semiconductor devices*. Singapore: World Scientific, 2005. ISBN 978-981-256-395-8.
- [9] BISHOP, J. W. Microplasma Breakdown and Hot-spots in Silicon Solar-Cells. *Solar Cells*. 1989, vol. 26, no. 4, pp. 334-349. ISSN 0379-6787.
- [10] GRMELA, L., P. SKARVADA, P. TOMANEK, R. MACKU and S. SMITH. Thermal dependence of light emission from reverse-biased monocrystalline silicon solar cells. *Solar Energy Materials and Solar Cells*. 2012, vol. 96, no. 1, pp. 108-111. ISSN 0927-0248.

## About Authors

**Robert MACKU** was born in 1982. He received his M.Sc. from Electronics and Communication technique in 2007, and Ph.D. from Physical Electronic and Nanotechnology in 2012. His research interests include semiconductor physics and application of noise diagnostic methods to solar cells.

**Pavel KOKTAVY** was born in 1972. His is Associate Professor at Department of Physics, Faculty of Electrical Engineering and Communication, Brno University of Technology. He received his M.Sc. from Cybernetics and Biomedical Engineering in 1995, and two Ph.D. from Physics of Condensed Matter and Acoustics in 2001 and Microelectronics and Technology in 2002. His research activities include fluctuation processes in solid states, diagnostics of semiconductor devices, problems of diagnostics and ageing of insulating materials and usage of electromagnetic and acoustic emission for diagnostics of cracks in mechanically loaded insulating materials.

**Jiri SICNER** was born in 1987. He received his M.Sc. from Communications and Informatics in 2011. His research interests include non-destructive diagnostic of solar cells and photonic components.